Dependence of the configurational entropy on amorphous structures of a hard-sphere fluid

Arijit Mondal, Leishangthem Premkumar, and Shankar P. Das*
School of Physical Sciences, Jawaharlal Nehru University, New Delhi 110067, India
(Received 7 March 2017; revised manuscript received 6 June 2017; published 12 July 2017)

The free energy of a hard-sphere fluid for which the average energy is trivial signifies how its entropy changes with packing. The packing η_f at which the free energy of the crystalline state becomes lower than that of the disordered fluid state marks the freezing point. For packing fractions $\eta > \eta_f$ of the hard-sphere fluid, we use the modified weighted density functional approximation to identify metastable free energy minima intermediate between uniform fluid and crystalline states. The distribution of the sharply localized density profiles, i.e., the inhomogeneous density field $\rho(\mathbf{x})$ characterizing the metastable state is primarily described by a pair function $g_s(\eta/\eta_0)$. η_0 is a structural parameter such that for $\eta = \eta_0$ the pair function is identical to that for the Bernal random structure. The configurational entropy $\mathcal{S}_c$ of the metastable hard-sphere fluid is calculated by subtracting the corresponding vibrational entropy from the total entropy. The extrapolated $\mathcal{S}_c$ vanishes as $\eta \to \eta_K$ and η_K is in agreement with other works. The dependence of η_K on the structural parameter η_0 is obtained.

DOI: 10.1103/PhysRevE.96.012124

I. INTRODUCTION

The pioneering computer simulation studies by Alder and Wainwright [1,2] and others [3,4] showed that a system of purely repulsive hard spheres with periodic boundary conditions upon "cooling"[5] can exist in both a disordered fluid state and an ordered crystalline state. For the hard-sphere system the temperature is trivially its average kinetic energy, and the relevant thermodynamic variable is the density or, equivalently, the packing fraction η [6]. Upon increasing the packing fraction η of the disordered fluid, a phase transition occurs at $\eta = \eta_f = 0.494$ to a crystalline state in which the average position of the hard spheres form a face-centered cubic (fcc) lattice [7]. For $\eta > \eta_f$, the supercooled hard-sphere fluid crystallizes [8], with the process getting faster as the "undercooling" increases [9]. Conversely, upon lowering the packing fraction, the crystal melts to a fluid state at $\eta_m = 0.545$. These states are linked by first-order phase transition, with two phases coexisting between the packing fractions η_f and η_m. Later simulation studies [10] indicated that the hard-sphere system can also be brought to a metastable glassy state by adopting special schemes for compressing the equilibrium hard-sphere fluid to a supercooled fluid state. The formation of a long-lived glassy phase for hard-sphere-like colloidal suspensions has also been demonstrated [11] in experiments. This occurs at high densities, in addition to the equilibrium fluid and solid phases of such systems. Through extensive simulations of one-component systems of larger sizes, and up to longer times, the existence of the hard-sphere glassy state has also been questioned [12]. There is increasing evidence that monodisperse hard-sphere systems do not form a stable glassy phase [13,14] and a small amount of spread in the size of the particles, referred to as polydispersity, actually avoids the crystallization, keeping the system in a metastable "supercooled" state. For example, the undercooled fluid state has been studied by using a binary mixture of equal mass with a size ratio of 0.905, with the corresponding $\eta_f = 0.506$ and $\eta_m = 0.548$ [8]. The interesting point here is that the observed equilibrium phase behavior of this polydisperse system could be accurately mapped to that predicted for a one-component hard-sphere system by computer simulation.

The hard-sphere crystal has an anomalous lattice dynamics which is entirely controlled by collisions. The motion of the freely moving hard spheres in the crystal between collisions is ballistic. In this respect the ordered state is analogous to the low-density fluid in which the particles are largely moving ballistically and collisions are infrequent. Using a classical density functional theory (DFT) approach, the equilibrium state is identified as a minimum of a free energy functional being treated as a function of the inhomogeneous density $\rho(\mathbf{x})$. The minimized value of this functional reduces to an appropriate thermodynamic property of the system depending on the ensemble used to describe the many-particle system [15,16]. For a grand canonical ensemble description, the minimum value is the grand potential Ω. This is particularly useful in the study of the coexistence of different phases. Similarly in a canonical ensemble description of the particles, the corresponding quantity at minimum is the Helmholtz free energy $\mathcal{F}$ of the system. In the present work we use the modified weighted density functional approximation (MWDA) to evaluate the Helmholtz free energy [17]. This is useful for our primary interest, which is the entropy for stable or metastable states. We mark the freezing transition point η_f as the packing fraction at which $\mathcal{F}$ for the fcc crystalline state is lower than that for the disordered fluid state [17].

For decay of fluctuations in the metastable liquid, the relaxation time τ_α increases sharply with increasing η, and as the extent of "supercooling" increases, a qualitative crossover in its dynamics is observed. A characteristic thermodynamic property of the metastable fluid in terms of which this crossover in relaxation behavior is expressed is its configurational entropy $\mathcal{S}_c$. The latter signifies large-scale motion of the constituent particles in the metastable state and decreases with increasing particle localization. The definition of $\mathcal{S}_c$, however, is not unique, and in the past it has been estimated using several approaches [18–21]. From an experimental viewpoint [22], it is estimated from the total entropy by subtracting

*shankar0359@yahoo.com

the contribution coming from the vibrational motions of the constituent particles of the fluid. Other definitions rely on the free energy landscape paradigm. As η becomes much higher than η_f, a large number of local minima appears in the free energy landscape for the many-particle system. The configurational entropy of a metastable system has been estimated [23] as the logarithm of the number of such metastable free energy minima at a given η. With increasing η, the individual free energy minima become deeper and fewer in number. If the number of such minima is subexponential, the configurational entropy per particle goes to 0. This definition of $\mathcal{S}_c$ has been used in computational methods [24], as well as in replica theory [25,26]. In the latter, the partition function for the structural glass in the absence of any intrinsic disorder is evaluated in terms of n weakly coupled replicas of the original system and taking, finally, the $n\to 1$ limit.

For the case of hard spheres which we consider here, estimation of the entropies is somewhat special [27] since the energy is irrelevant in this case and is simply equal to $\frac{3}{2}k_BT$, the potential contribution being 0. In this case the fluid-crystal transition is completely driven by the entropy. Thus above η_f, the crystal entropy is *higher* than that of the fluid. This would imply that the configurational entropy, when defined as the difference between the fluid and the crystal entropies, is negative at all $\eta > \eta_m$. In the present work the configurational entropy for the metastable hard-sphere fluid is taken as the difference between the total entropy $S_{\rm tot}$ and the corresponding vibrational entropy $S_{\rm vib}$ for the amorphous state. $S_{\rm tot}$ for the hard-core system is obtained from the total free energy of the fluid. In the metastable state, vibration of the particles is around a frozen amorphous structure which persists over the time scale of structural relaxation. The vibrational contribution to the entropy $\mathcal{S}_v$ is obtained here from the ideal-gas part of the free energy $F_{\rm id}$.

Our primary focus here is on the deeply supercooled state for η much higher than η_f. For the crystalline state the close-packed fcc structure of a hard-sphere system is $\eta_c = 0.740$. However, for a random structure this is unsettled. Generally the closest random close-packing value has been found to be 0.62–0.64 in different studies. This state has often been linked to an underlying ideal glass transition in the metastable hard-sphere fluid characterized by the vanishing of the configurational entropy. A similar [28] transition in a hard-sphere system has also been predicted in dynamic models [29–31] in terms of ergodicity to nonergodicity and are characterized by order parameters with scaling behavior [32,33]. Here using a (modified) weighted density functional approach [34], which has been very successful in understanding the freezing transition from the homogeneous liquid to the crystalline state, we calculate the configurational entropy of the metastable hard-sphere fluid with a random structure. In particular, our study shows how $\mathcal{S}_c$ depends on the type of amorphous structure that characterizes the mass localization in the metastable fluid. The "entropy crisis" which occurs in the metastable liquid with increasing η and vanishing $\mathcal{S}_c$ constitutes a primary issue in understanding the physics of the glass transition [35]. The paper is organized as follows: In Sec. II, we describe briefly the MWDA model for computing the total free energy and hence the total entropy $\mathcal{S}_{\rm tot}$ for the amorphous metastable fluid. In Sec. III we compute the vibrational contribution to the entropy $\mathcal{S}_{\rm vib}$. Subtracting out the vibrational part from the total entropy, we obtain $\mathcal{S}_c$ and the corresponding numerical results are given in Sec. III. We end the paper with a short discussion of our results in Sec. IV.

II. THE DENSITY FUNCTIONAL MODEL

In the classical DFT the free energy of the inhomogeneous solid is obtained in terms of a density expansion around the uniform liquid state [16,36,37]. The inhomogeneous density $\rho(\mathbf{x})$ is treated as the order parameter and is expressed in terms of localized Gaussian profiles, respectively, peaked around a set of points $\{\mathbf{R}_i\}$ of a lattice which may represent an ordered crystal [38] or a disordered amorphous system [39–43]. These strongly localized density profiles signify the constituent particles vibrating around the respective points on $\{\mathbf{R}_i\}$. In the so-called modified weighted density functional approximation [17] the free energy of the solid, treated as a function of $\rho(\mathbf{x})$, is calculated by mapping the inhomogeneous system to an equivalent homogeneous liquid of lower density. The structural information on the uniform liquid state, as well as the underlying lattice $\{\mathbf{R}_i\}$ depicting the crystalline or the amorphous state, is required in the MWDA calculation as inputs. This is an effective medium approach which is particularly suitable for hard-sphere systems. We elaborate on this further in the discussion section Sec. IV).

In the following the formulas used in the subsequent section for numerical computation are stated without derivation; for this we refer the reader to the standard literature [44–46]. The free energy functional $F[\rho]$ of the liquid is obtained as the sum of two parts, $F[\rho] = F_{\rm id}[\rho] + F_{\rm ex}[\rho]$, where $F_{\rm id}$ and $F_{\rm ex}$ denote the ideal-gas and the interaction contributions, respectively. The density $\rho(\mathbf{x})$ is approximated as the sum of Gaussian profiles located at the points of a lattice $\{\mathbf{R}_i\}$:

$$\rho(\mathbf{r}) = \sum_{i=1}^{N} \left(\frac{\alpha}{\pi}\right)^{\frac{3}{2}} e^{-\alpha|\mathbf{r}-\mathbf{R}_i|^2} \equiv \sum_{i=1}^{N} \phi(\mathbf{r}-\mathbf{R}_i). \tag{1}$$

α is the width parameter of the Gaussian function $\phi(\mathbf{r})$. The $\alpha\to 0$ limit corresponds to a uniform liquid. A large α corresponds to a strongly localized density profile. For describing the glassy state the $\{\mathbf{R}_i\}$ values are distributed randomly. The ideal-gas part $F_{\rm id}$ of the free energy for the nonuniform density $\rho(\mathbf{x})$ is a simple generalization of the corresponding free energy expression for the uniform density. $F_{\rm id}$ per particle in units of $\beta(=1/k_BT)$ is denoted $f_{\rm id}$,

$$f_{\rm id}[\rho(\mathbf{r})] = N^{-1}\int d\mathbf{r}\rho(\mathbf{r})(\ln[\rho(\mathbf{r})\Lambda^3] - 1), \tag{2}$$

where Λ is the thermal De Broglie [47] wavelength arising from the momentum integration in the partition function. Using the parametric form, (1), for the density $\rho(\mathbf{x})$, Eq. (2) obtains the free energy as a function of the width parameter α. For the large α corresponding to very localized density distributions, the summation over all lattice sites in $\rho(\mathbf{r})$ is approximated in terms of the contribution from the nearest site. With this approximation Eq. (2) reduces to

$$f_{\rm id}(\alpha) \approx -\frac{5}{2} + 3\ln\left(\sqrt{\frac{\alpha}{\pi}}\Lambda\right). \tag{3}$$

This expression for the ideal-gas free energy for the inhomogeneous system is also obtained by assuming the localized state with density profiles as a collection of noninteracting harmonic oscillators with a density of states following the Debye distribution. We discuss this in Appendix A. In the following Λ and α are scaled in terms of the basic length scale σ (hard-sphere diameter) for the fluid. We denote $\tilde{\Lambda} = \Lambda/\sigma$ and $\alpha^* = \alpha\sigma^2$. We keep $\tilde{\Lambda} = 1.0$ throughout this paper, to maintain similarity to previous works [21,41].

In weighted density functional theory [48] a coarse-grained form $\bar{\rho}(\mathbf{x})$ of the strongly localized density profile $\rho(\mathbf{x})$ is obtained by averaging over a local volume,

$$\bar{\rho}(\mathbf{x}) = \int d\mathbf{x}' w[\mathbf{x} - \mathbf{x}'; \bar{\rho}(\mathbf{x})]\rho(\mathbf{x}'). \tag{4}$$

$w(\mathbf{x} - \mathbf{x}')$ is a weight function over the relevant region around point $\mathbf{x}'$ of the physical density $\rho(\mathbf{x}')$. $F_{\rm ex}$ is expressed as an integral of the free energy $\tilde{f}_{\rm ex}$ per particle evaluated for a weighted density $\bar{\rho}$,

$$\beta F_{\rm ex}[\rho] = \int d\mathbf{x}\rho(\mathbf{x})\tilde{f}_{\rm ex}[\bar{\rho}(\mathbf{x})]. \tag{5}$$

In the MWDA [17], the excess part of the free energy per particle $\tilde{f}_{\rm ex}(\hat{\rho})$ is expressed as a function of the globally weighted density $\hat{\rho}$,

$$\hat{\rho} = \frac{1}{N}\int d\mathbf{x}\rho(\mathbf{x})\int d\mathbf{x}'\rho(\mathbf{x}')w(\mathbf{x} - \mathbf{x}'; \hat{\rho}). \tag{6}$$

The key equation of the MWDA is a self-consistent integral equation [17] involving the weighted density $\hat{\rho}$ or, equivalently, the corresponding packing fraction $\hat{\eta} = \pi\hat{\rho}\sigma^3/6$ in terms of the suitably chosen free energy function $f_{\rm ex}(\hat{\eta})$:

$$2f'_{\rm ex}(\hat{\eta})\hat{\eta} = -\eta\hat{\eta}f''_{\rm ex}(\hat{\eta}) - N^{-1} \int d\mathbf{x}\int d\mathbf{x}'\rho(\mathbf{x})\rho(\mathbf{x}')c(|\mathbf{x} - \mathbf{x}'|; \hat{\eta}). \tag{7}$$

This gives rise to the following self-consistent equation for the packing fraction of the effective liquid in the MWDA,

$$\hat{\eta} = \mathcal{I}(\hat{\eta},\alpha)(2f'_{\rm ex}(\hat{\eta}) + \eta f''_{\rm ex}(\hat{\eta}))^{-1} \equiv F(\eta). \tag{8}$$

The single and double primes over $f_{\rm ex}(x)$ in the above equation denote, respectively, the first and second derivatives of the function with respect to its argument x. Evaluation of the second term on the right-hand side of Eq. (8) involving the integral $\mathcal{I}$ in terms of the width parameter α of the density function $\rho(\mathbf{x})$ is discussed in Appendix B. To solve Eq. (8), the functional form of the free energy $f_{\rm ex}(\eta)$ is taken from the Percus-Yevick (PY) expression of the excess free energy of a hard-sphere system [47],

$$f_{\rm ex}(\eta) = \frac{3}{2}\left[\frac{2\eta - \eta^2}{(1-\eta)^2}\right] - \ln(1-\eta). \tag{9}$$

For the direct correlation function $c(r)$ we use the corresponding solution [49,50] of the PY equation for a hard-sphere system [51]. The solution of this self-consistent MWDA equation for a chosen value of the parameter α is illustrated in Fig. 1.

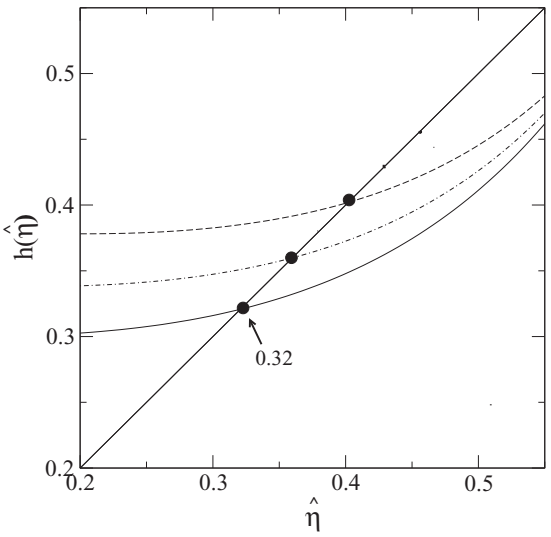

FIG. 1. Solution of the self-consistent equation of the MWDA for packing fraction $\eta = 0.539$ and $\alpha = 100$. We plot the right-hand side of Eq. (8) along the y axis vs $\hat{\eta}$ to mark its transection point with the $y = \hat{\eta}$ line as the solution.

III. THE METASTABLE STATE

The total free energy per particle is obtained as the sum of the two parts given, respectively, by Eqs. (3) and (9),

$$f_{\rm tot} = f_{\rm id}(\alpha) + f_{\rm ex}[\hat{\eta}(\alpha)]. \tag{10}$$

For a fixed value of η, the total free energy is calculated over a range of the width parameter α values by solving the MWDA equation in each specific case. The minimum of the free energy with respect to the parameter α is at $\alpha = \alpha_{\rm min}$ and determines the free energy as well as the optimum density distributions for the equilibrium state. Successful applications of this method have been made for understanding the freezing of hard-sphere systems [17]. The metastable amorphous state, distinct from the uniform liquid state, is identified by locating the intermediate minimum of the corresponding free energy with respect to the mass localization parameter α. In Fig. 2 the dependence of the free energy on the localization parameter is shown. The metastable minimum of the total free energy calculated using the DFT is displayed for four values of η ranging from 0.539 to 0.561. In all cases the corresponding amorphous structure $\{\mathbf{R}_i\}$ is chosen for $\eta_0 = 0.68$. The parameter η_0 introduced in Eq. (B2) characterizes the underlying structure on which mass localization occurs. The position of the minimum at $\alpha_{\rm min}$ is indicated by the arrow. The free energies of the corresponding crystalline states are shown in the inset in Fig. 2 for the same η values as in the main panel. In the metastable state with a random $\{\mathbf{R}_i\}$, the free energy is higher than that of the corresponding fcc structure. The η dependence of the localization parameter $\ell = 1/\sqrt{\alpha_{\rm min}}$ (scaled with respect to the hard-sphere diameter σ) corresponding to the metastable minimum of the free energy is shown in Fig. 3. We find that $\alpha_{\rm min}$ is an increasing function of η. With an increase in η, the particles become more localized and hence the amplitudes of vibration of the particles around their respective mean position fall.

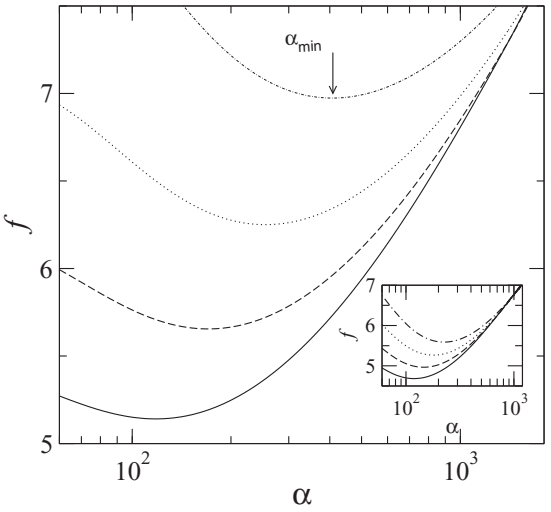

FIG. 2. Metastable minimum of the total free energy as a function of the localization parameter α for packing fraction $\eta = 0.539$ (solid line), 0.56 (dashed line), 0.581 (dotted line), and 0.602 (dot-dashed line), corresponding to the amorphous structures characterized by $\eta_0 = 0.69$, and for the fcc crystalline structure (inset). The position of the minimum at α_{min} in each case is shown by the arrow.

A. Configurational entropy

The configurational entropy $\mathcal{S}_c$ of the amorphous metastable state is obtained here as the difference between the total entropy and the corresponding vibrational entropy of the metastable hard-sphere fluid. The total entropy expressed in units of k_B is

$$\mathcal{S}_{\rm tot} = \tfrac{3}{2} - f_{\rm tot}, \tag{11}$$

where the total free energy $f_{\rm tot}$ is obtained from DFT. For calculation of the vibrational entropy, we note that in the DFT model, the individual Gaussian density profiles are interpreted as particles vibrating around the respective lattice points $\mathbf{R}_i$. Compared to the homogeneous liquid state there is a reduction

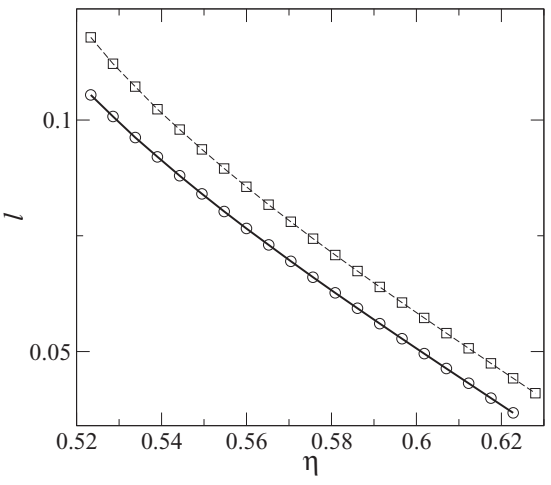

FIG. 3. Localization length (in units of hard-sphere diameter σ) for the metastable glassy state, $\ell = 1/(\sqrt{\alpha_{\rm min}}\sigma)$, vs packing fraction η. The parameter η_0, characterizing the underlying amorphous structure equals 0.69 (solid line) and 0.68 (dashed line).

in entropy due to localization of the particle. This is clear from the expression for the ideal-gas part of the free energy for the inhomogeneous density distribution $\rho(\mathbf{x})$, given by Eq. (2). For large α the density profiles are sharply localized, obtaining the ideal-gas contribution as [48]

$$s_{\rm id}(\alpha) = \tfrac{3}{2} - f_{\rm id}(\alpha). \tag{12}$$

The vibrational contribution to the entropy for an inhomogeneous fluid with localized density profiles of width α is obtained by subtracting from the ideal-gas entropy the corresponding uniform density limit $s^0_{\rm id}$:

$$\mathcal{S}_{\rm vib}(\alpha) = s_{\rm id}(\alpha) - s^0_{\rm id}. \tag{13}$$

Using $s^0_{\rm id} = 3/2 - f^0_{\rm id}$, where $f^0_{\rm id}$ is the ideal-gas free energy of the uniform fluid, the vibrational entropy $\mathcal{S}_{\rm vib}(\alpha)$ is estimated. The above definition of vibrational entropy implies that there is no vibrational contribution in the homogeneous state. Using Eqs. (10), (11), and (13) we obtain that the configurational entropy of the amorphous state corresponding to the mass localization parameter α is

$$\mathcal{S}_c(\eta) = \mathcal{S}_{\rm tot}(\eta) - \mathcal{S}_{\rm vib}(\eta) = -(f_{\rm ex} + \ln\eta) + \mathcal{C}_0, \tag{14}$$

where $\mathcal{C}_0 = 5/2 + \ln(\pi/6)$. We calculate $\mathcal{S}_c$ corresponding to the packing fraction η lying in the range 0.539 to 0.601. The configurational entropy S_c of the hard-sphere system is determined here using two inputs. First, the amorphous structure $\{\mathbf{R}_i\}$ for the centers of the Gaussian density profiles characterizing the inhomogeneous mass distribution is used. This is expressed in terms of the Bernal pair distribution function [52]. The parameter η_0 introduced in Eq. (B2) characterizes the underlying amorphous structure. Second, we use the correlations of the uniform liquid state determined by the packing fraction η. For a given η we first calculate the $\alpha = \alpha_{\rm min}$ at which the total free energy $f_{\rm tot}$ is minimum. Then using Eq. (14) we calculate $\mathcal{S}_c$. The point at which the extrapolated $\mathcal{S}_c$ goes to 0 is the so-called Kauzmann point. The dependence of $\mathcal{S}_c$ on η is displayed in Fig. 4. The same figure also shows a comparison with the results for the configurational entropy calculated using the replica approach [53,54], overlap models [24], and potential energy landscape models [21]. We obtain the same $\eta_{\rm K}$ as in Ref. [53] with the choice $\eta_0 = 0.703$. The two curves showing the corresponding S_c vs η are obtained with the respective pair functions $g_s(r)$ shown in Fig. 5. The present model shows how $\eta_{\rm K}$ depends on the structural parameter η_0, which characterizes the underlying amorphous structure $\{\mathbf{R}_i\}$ of the Gaussian profiles of the inhomogeneous density distribution. This result is shown in Fig. 6.

We now consider the density dependence of the entropy of the metastable amorphous state with respect to that of the fcc crystal. As pointed out, for $\eta > \eta_m$ the total entropy of the hard-sphere crystal is *higher* than that of the corresponding amorphous state. The difference $\Delta\mathcal{S}_{\rm tot} = \mathcal{S}_{\rm tot} - \mathcal{S}_{\rm fcc}$ between the entropy of the metastable amorphous state and that of the crystalline state is therefore negative above η_m. We show in Fig. 7 the $\Delta\mathcal{S}_{\rm tot}$ vs η plot. The corresponding difference obtained in terms of the vibrational entropy $\Delta\mathcal{S}_{\rm vib} = \mathcal{S}_{\rm vib} - \mathcal{S}_{\rm fcc}$ is also shown in the inset in Fig. 7. This is a property, of course, specific to the hard-sphere crystal, in which the

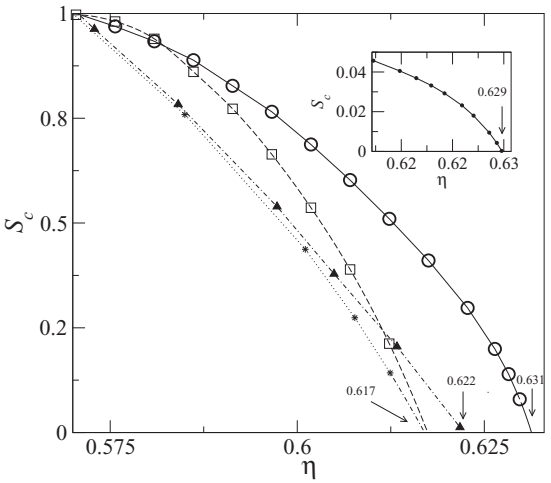

FIG. 4. The configurational entropy $\mathcal{S}_c$ measured with respect to its value at η_K vs the packing fraction η. The present model with amorphous structures corresponds to $\eta_0 = 0.703$ (solid line), 0.693 (dashed line), Ref. [53] (dotted line), and Ref. [21] (dot-dashed line). The η_K value in each case is shown by the corresponding arrow. Inset: Results of S_c vs η from Ref. [24].

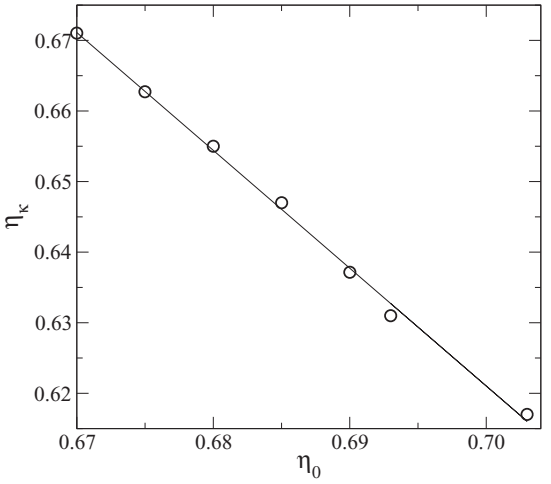

FIG. 6. Plot of the critical packing fraction η_K for which the metastable hard-sphere fluid reaches the highest entropy vs the corresponding structural parameter η_0 depicting the amorphous lattice for the metastable state.

ordered state is similar to a low-density fluid in certain respects. We discuss this point further in the next section. Finally, from the nature of the density dependence of $\mathcal{S}_c(\eta)$, we note that at an intermediate density, $\eta_m < \eta_{\max} < \eta_K$, the configurational entropy reaches a maximum. These results all correspond to amorphous structures described in terms of the pair function characterized by a specific value of the η_0 introduced in Eq. (B2). In Fig. 8 we show how the corresponding packing fraction $\eta_{\max}$ changes with the corresponding structural parameter η_0. The inset shows how the maximum $\mathcal{S}_c^{\max}$ of S_c at $\eta = \eta_m$ changes with the structural parameter η_0.

In the MWDA approach the free energy of the amorphous solid is obtained by mapping the inhomogeneous hard-sphere crystal to an equivalent fluid of much lower density $\hat{\rho}$. Use of the input structure function for a uniform liquid in the present DFT calculation occurs twice. First, we use the Percus-Yevick expression for the direct correlation function $c(r)$ for the hard-sphere potential in solving the MWDA equation and obtain the density $\hat{\rho}$. Second, the free energy for the solid is obtained by evaluating the standard PY free energy expression at density $\hat{\rho}$. Using PY expressions in both steps maintains consistency. Also, keeping in mind the fact that the success of the MWDA approximation for hard-sphere crystals is linked to the ballistic nature of the particle motion for the discontinuous

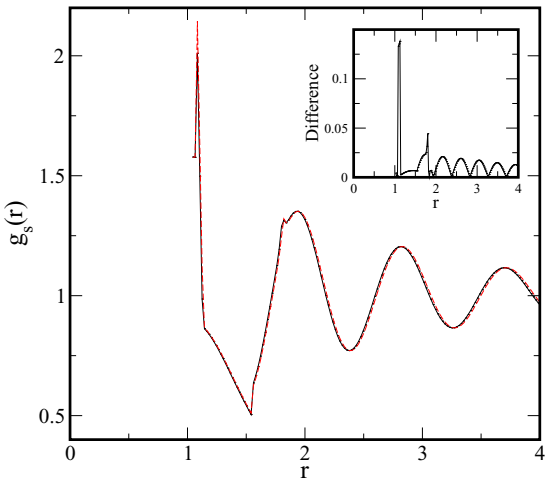

FIG. 5. Pair function $g_s(r)$ (see text) used in the present model with amorphous structures corresponding to $\eta_0 = 0.703$ (solid line) and 0.693 (dashed line) to obtain the corresponding S_c curves in Fig. 4.

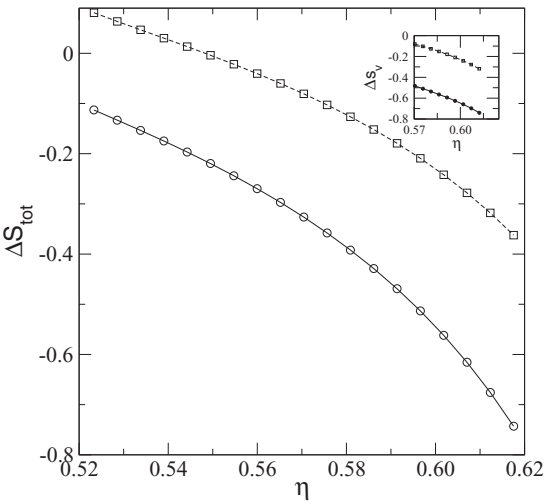

FIG. 7. The difference $\Delta\mathcal{S}_{\text{tot}}$ of the total entropy of a hard-sphere system in the metastable amorphous state from that of the fcc crystalline state vs the corresponding packing fraction η. The dashed line correspond to results for the parameter value $\eta_0 = 0.693$, while the solid line represents $\eta_0 = 0.703$. For a hard-sphere fluid this is always negative. Inset: Difference between the corresponding vibrational part of the entropy of the amorphous state and the crystal entropy.

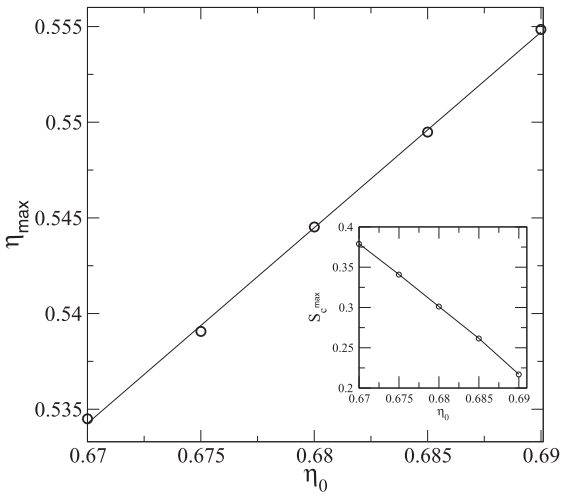

FIG. 8. The packing fraction η_{max} at which the maximum of $\mathcal{S}_c$ occurs vs the structural parameter η_0. Inset: How $\mathcal{S}_c^{max}$ changes with the structural parameter η_0.

potential, we avoid adding an empirical tail to $c(r)$ using the Verlet-Weis (VW) correction [55]. Furthermore, the difference between the PY structure factors obtained with and those obtained without VW correction, respectively, is prominent only at high densities. We show in Fig. 9 how the direct correlation functions $c(r)$ obtained from the PY solution with and without VW correction, respectively, change with the distance r for a typical packing fraction value $\hat{\eta} = 0.338$.

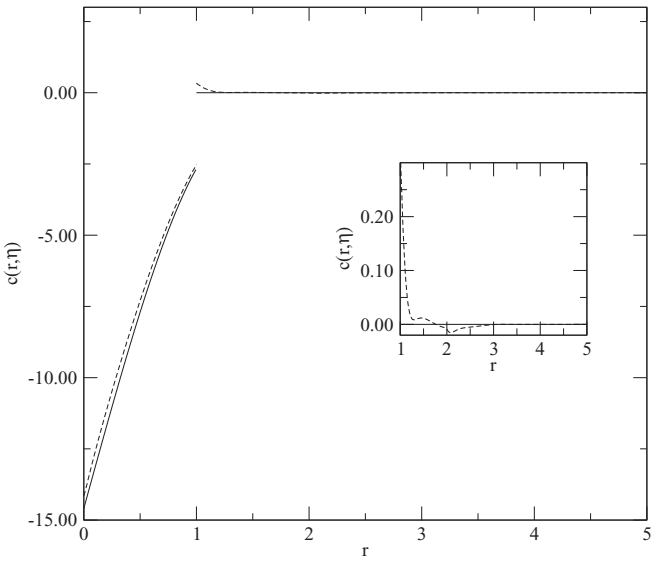

FIG. 9. The direct correlation functions $c(r)$ obtained from the PY solution with Verlet-Weiss corrections (dashed line) and without Verlet-Weiss corrections (solid line), respectively, vs the radial distance r/σ for a typical packing fraction value $\hat{\eta} = 0.338$ corresponding to the solution of the self-consistent MWDA equation. Inset: $r > \sigma$ part of the self-consistent MWDA equation on a magnified scale.

IV. DISCUSSION

We work here with a model of a metastable liquid in which the inhomogeneous density is expressed as a collection of Gaussian profiles centered around sites distributed on an amorphous lattice. In the coarse-grained description these density profiles represent particles oscillating around the respective sites. At high densities, the particles get trapped inside the cage made by its neighbors for increasingly longer times [56,57] and perform vibrational motion around sites which form an amorphous lattice. Indeed such a state is needed to justify the existence of transverse sound waves in amorphous solids [58,59]. The weighted density approximation is appropriate only for a hard-core system, which also makes the present DFT calculation of $\mathcal{S}_c$ applicable only for a hard-sphere fluid. Keeping up to second order in density fluctuations, the MWDA describes quite accurately hard-core systems in terms of an equivalent uniform low-density fluid. Hard spheres in the crystal move freely between collisions and are very much like the constituent particles in the low-density fluid. Indeed for purely hard-core repulsive systems, no expansion for the Hamiltonian in terms of displacements from equilibrium sites exists. The lattice dynamics is entirely controlled by collisions and the motion of the particles between the collisions loses coherence very rapidly. This peculiarity is the reason for the success of the MWDA as an accurate tool for computation of the thermodynamic properties of the strongly inhomogeneous hard-sphere crystal in terms of those of an equivalent low-density fluid. In the case of softer potentials, this analogy, however, does not hold. For the $1/r^n$-type potential (where $n \to \infty$ is the hard-sphere potential), as n approaches values more typical of short-range interactions in real systems, the coherence in the motion of the particles increases. Therefore with softer potentials the above similarity between the low-density liquid and the solid is absent, and as a result, the weighted density functional theories are less successful for understanding fluids with softer interactions. In addition, for the hard-sphere crystal the average domain of motion of a particular sphere is constrained in space over a scale determined largely by the range of the direct correlation function $c^{(2)}(r)$ at the corresponding density. The range of the direct correlation function increases considerably with that of the interaction potential (n becoming smaller). Hence the coarse-graining length scale of the weighted density over which the inhomogeneous density should be averaged sharply increases. It would possibly be appropriate to include higher-order correlations like $c^{(3)}$ in the calculation of the weight function for softer potentials and hence to use the DFT approach for such fluids.

For calculation of the thermodynamic properties of inhomogeneous fluids, various forms of the weighted density functional approach have been proposed. The fundamental measure theory [60,61] is an important development in the study of static correlation functions for a dense fluid. In the present work our primary focus is on the glassy state and calculation of the configurational entropy. We study the free energy in terms of the MWDA in which the high-density system is mapped to an equivalent uniform fluid of much lower density. For estimating the thermodynamic properties of the latter, we use the PY solution since the latter is reliable at

such low densities. Here the fundamental measure theory for the uniform hard-sphere system matches with the PY theory and one can adopt the fundamental measure theory as a further improvement.

At deep supercooling or farther away from the freezing density, the metastable states corresponding to inhomogeneous density only occurs for very large width parameter values $\alpha_{\min}$. In such cases of highly localized density profiles, the packing $\hat{\eta}$ of the equivalent liquid of MWDA is much lower than the average packing η. Hence using the Percus-Yevick formula for $f_{\rm ex}$ works well here. As pointed out above, for the hard-sphere system, the total entropy of the crystal is higher than that of the amorphous state above melting density. Since the configurational entropy of the hard-sphere crystal is 0, its vibrational entropy has to be *higher* than that of the amorphous state. Indeed for the hard-sphere fluid the optimum width parameter $\alpha_{\min}$ corresponding to the crystal structure should be *less* than that for the amorphous metastable state.

The present calculation of $\mathcal{S}_c$ using DFT is based on an interpretation of the model different from some of the other DFT-based models [62]. The free energy calculation done here does not refer to one single aperiodic distribution of the particles. With the Bernal pair function as the structural input, we interpret the free energy as being averaged over a set of random distributions. Hence the corresponding configurational entropy $\mathcal{S}_c$ computed using this free energy is also relevant as a thermodynamic property. Moreover, for sharply localized density profiles, corresponding to high values of the width parameter α we apply the MWDA approach and not the low-order expansion of the free energy used in previous works [39,41,63,64]. As pointed out above the MWDA is only appropriate for hard-sphere systems, unlike the case of softer potentials [65]. For the Ramakrishnan-Yousuff free energy expansion, on the other hand, it was shown that for intermediate densities close to the freezing point (η_m), a metastable minimum for the amorphous structure exists. In this case the width parameter $\alpha_{\min}$ is definitely lower than that for the crystal [66–69]. However, breaking the total entropy into clearly separable vibrational and configurational parts is not viable for such low-α minima. These metastable structures with a low degree of mass localization signify heterogeneous density profiles and possibly signatures of a liquid-liquid-type transition in the metastable liquid below the freezing point.

ACKNOWLEDGMENTS

S.P.D. and A.M. acknowledges Project No. 2011/37P/47/BRNS of DAE, India for financial support. A.M. acknowledges UGC-BSR, India and L.P. acknowledges CSIR, India for financial support. S.P.D. acknowledges for financial support Jawaharlal Nehru University's UPE-II Grant, funded by UGC, India.

APPENDIX A: THE VIBRATIONAL MODES

Next we calculate the contribution to the entropy from harmonic modes in a hard-sphere crystal with a Debye distribution. The vibrational modes are taken as harmonic modes of frequencies ω_i, with $i = 1, \ldots, N$. The partition function of the system of N independent harmonic oscillators is given by

$$\mathcal{Z}_N^V = \prod_{\omega_i=1}^{3N} \sum_{n_i=1}^{\infty} \exp\left[-\frac{\hbar\omega_i}{k_B T}\left(n_i + \frac{1}{2}\right)\right]. \tag{A1}$$

The corresponding vibrational contribution to the free energy is obtained as

$$F_v = -k_B T \ln \mathcal{Z}_N^V = \int \ln(1 - e^{-\beta\hbar\omega}) g(\omega) d\omega. \tag{A2}$$

We have ignored a temperature-independent part coming from the zero-point energy of the harmonic modes. $g(\omega)$ is the vibrational density of states. Using the standard thermodynamic relation, expressing the entropy as a derivative of the corresponding free energy at fixed volume, the contribution to entropy in units of k_B is obtained as

$$\mathcal{S}_v = \int_0^{\omega_D} \left[-\ln(1 - e^{-\beta\hbar\omega}) + \frac{\beta\hbar\omega}{e^{\beta\hbar\omega} - 1}\right] g_D(\omega) d\omega. \tag{A3}$$

The density of states $g(\omega)$ is assumed here to be the Debye distribution $g_D(\omega)$, which is nonzero to an upper cutoff of ω_D:

$$\begin{aligned} g_D(\omega) &= \frac{9N}{\omega_D^3}\omega^2 \quad \text{for} \quad \omega < \omega_D, \\ &= 0 \qquad\quad \text{for} \quad \omega > \omega_D. \end{aligned}$$

The entropy per particle is obtained as

$$s_{\rm ho} = -3\ln(1 - e^{-x_D}) + \frac{12}{x_D^3}\int_0^{x_D} \frac{x^3 dx}{e^x - 1}. \tag{A4}$$

The upper cutoff of frequency $x_D = \beta\hbar\omega_D$ is here identified using the density functional model. We take the free energy of these noninteracting harmonic oscillators as $f_{\rm id} = (3/2) - s_{\rm ho}$. Evaluating the integral on the right-hand side of Eq. (A4) in the limit $x_D \ll 1$ to leading order, $f_{\rm id}$ reduces to the asymptotic expression, (3), if we identify the upper cutoff

$$x_D = \sqrt{\alpha/\pi}\,\Lambda. \tag{A5}$$

Relation (A5) is, however, a generalization and is based on qualitative considerations. It links two equivalent descriptions for the vibrational modes in the solid, namely, the continuum density functional theory in terms of Gaussian density profiles and the microscopic model of harmonic modes having a Debye density of states. The microscopic result becomes identical to the corresponding DFT expression for large values of the parameter α for the limit $x_D \ll 1$. The primary reason for this matching lies in the harmonic and Gaussian approximations in the respective models. For the amorphous solid, we generalize here the above relation to large x_D values as well. The Gaussian density profile in DFT represents a vibrating particle whose mean square displacement is proportional to α^{-1}. Thus a large α signifies increased localization, giving rise to vibrating modes with shorter wavelengths or larger wave vectors. Extrapolating dispersion relations for acoustic modes, this implies that the cutoff frequency x_D also increases. Keeping with this monotonic dependence we therefore extend the small-x_D relation.

APPENDIX B: THE MWDA EQUATION

The integral in the second term on the right-hand side of Eq. (8) involves products of densities at two points on $\{\mathbf{R}_i\}$. In the case of a crystalline structure, the lattice $\{\mathbf{R}_i\}$ is fixed by the corresponding crystalline symmetry. For the amorphous state we characterize this in terms of the pair correlation function $g_s(R)$ for a random lattice. Writing the densities at the two points $\mathbf{r}_1$ and $\mathbf{r}_2$ using Eq. (1), the integral $\mathcal{I}$ obtains two types of contributions involving indices (i, j), respectively, referring to the two particles, i.e., for $i = j$ and $i \neq j$. With the $i = j$ choice, there are N such terms, while for $i \neq j$ we introduce the pair distribution function $g_s(R)$ for the given structure. Equation (8) reduces to

$$\mathcal{I} = -\int d\mathbf{r}_1 \int d\mathbf{r}_2 \int d\mathbf{R} c(|\mathbf{r}_1 - \mathbf{r}_2|; \hat{\eta}) \phi(\mathbf{r}_1 - \mathbf{R})\phi(\mathbf{r}_2)\left[\delta(\mathbf{R}) + \frac{6\eta}{\pi} g_s(\mathbf{R})\right]. \tag{B1}$$

The pair distribution function $g_s(R)$ for a given separation R is written in terms of the Bernal pair distribution function $g_B(R)$ [52] through the scaling relation,

$$g_s(R) = g_B(\gamma_0 R), \tag{B2}$$

where $\gamma_0 = (\eta/\eta_0)^{1/3}$. The quantity η_0 is thus introduced here as a scaling parameter for the structure such that for packing fraction $\eta = \eta_0$ Bernal's structure [70] $g_B(R)$ is obtained. The mapping of the function from $R(\eta/\eta_0)^{1/3}$ to R makes the structure either dilute or contracted, depending on the scaling parameter η_0. The parameter η_0 crucially characterizes the dependence of the free energy landscape on the amorphous structure. With some trivial algebra the two terms on the right-hand side of Eq. (B1) reduce to

$$\mathcal{I} = A_1(\alpha) + \frac{24\hat{\eta}}{\gamma_0^2} \int_0^\infty dR R g_s(R) A_2(\alpha; R), \tag{B3}$$

where A_1 and A_2 are the integrals defined as

$$A_1(\alpha) = \sqrt{\frac{2\alpha^3}{\pi}} \int_0^\infty dr r^2 c(r; \hat{\eta}) e^{-\frac{\alpha}{2} r^2}, \tag{B4}$$

$$A_2(\alpha; R) = \sqrt{\frac{\alpha}{2\pi}} \int_0^\infty dr r c(r; \hat{\eta}) \times \left[e^{-\frac{\alpha}{2}(r-R)^2} - e^{-\frac{\alpha}{2}(r+R)^2}\right]. \tag{B5}$$

[1] B. J. Alder and T. E. Wainright, Phys. Rev. **127**, 359 (1962).
[2] B. J. Alder and T. E. Wainwright, J. Chem. Phys. **33**, 1439 (1960); **31**, 459 (1959).
[3] W. W. Wood and J. D. Jacobson, J. Chem. Phys. **27**, 1207 (1957).
[4] W. W. Wood and R. R. Parker, J. Chem. Phys. **27**, 720 (1957).
[5] J. M. Gordon, J. H. Gibbs, and P. D. Fleming, J. Chem. Phys. **65**, 2771 (1976).
[6] J. P. Dyre, J. Phys.: Condens. Matter **28**, 323001 (2016).
[7] W. G. Hoover and F. H. Ree, J. Chem. Phys. **49**, 3609 (1968).
[8] B. OMalley and I. Snook, Phys. Rev. Lett. **90**, 085702 (2003).
[9] S. R. Williams, I. K. Snook, and W. van Megen, Phys. Rev. E **64**, 021506 (2001).
[10] L. V. Woodcock, Ann. N.Y. Acad. Sci. **371**, 274 (1981).
[11] P. N. Pusey and W. van Megen, Nature (London) **320**, 340 (1986).
[12] S. R. Williams, P. McGlynn, G. Bryant, I. K. Snook, and W. van Megen, Phys. Rev. E **74**, 031204 (2006).
[13] I. Moriguchi, K. Kawasaki, and T. Kawakatsu, J. Phys. II France **5**, 143 (1995).
[14] M. D. Rintoul and S. Torquato, Phys. Rev. Lett. **77**, 4198 (1996); J. Chem. Phys. **105**, 9258 (1996).
[15] R. Evans, Adv. Phys. **28**, 143 (1979).
[16] S. P. Das, *Statistical Physics of Liquids at Freezing and Beyond* (Cambridge University Press, New York, 2011).
[17] A. R. Denton and N. W. Ashcroft, Phys. Rev. A **39**, 4701 (1989).
[18] R. J. Speedy, J. Chem. Phys. **110**, 4559 (1999).
[19] R. J. Speedy, J. Chem. Phys. **114**, 9069 (2001).
[20] T. Aste and A. Coniglio, Physica A **330**, 189 (2003).
[21] L. Angelani and G. Foffi, J. Phys. Condens. Matter **19**, 256207 (2007).
[22] A. W. Kauzmann, Chem. Rev. **43**, 219 (1948).
[23] R. Monasson, Phys. Rev. Lett. **75**, 2847 (1995).
[24] M. Cardenas, S. Franz, and G. Parisi, J. Chem. Phys. **110**, 1726 (1999).
[25] M. Mézard and G. Parisi, Phys. Rev. Lett. **82**, 747 (1999).
[26] V. Lubchenko and P. G. Wolynes, J. Chem. Phys. **119**, 9088 (2003)
[27] F. Zamponi and G. Parisi, Rev. Mod. Phys. **123**, 133501 (2005).
[28] L. Premkumar, N. Bidhoodi, and S. P. Das, J. Chem. Phys. **144**, 124511 (2016).
[29] U. Bengtzelius, W. Götze, and Sjolander, J. Phys. C. **17**, 5915 (1984).
[30] S. P. Das and G. F. Mazenko, Phys. Rev. E **79**, 021504 (2009).
[31] S. P. Das and G. F. Mazenko, J. Stat. Phys. **152**, 159 (2013).
[32] W. Götze, Z. Phys. B Cond. Matt. **60**, 195 (1985).
[33] S. P. Das, J. Chem. Phys. **98**, 3328 (1993).
[34] W. A. Curtin and N. W. Ashcroft, Phys. Rev. Lett. **56**, 2775 (1986).
[35] M. Mézard and G. Parisi, J. Phys.: Condens. Matter **12**, 6655 (2000).
[36] T. V. Ramakrishnan and M. Yussouff, Phys. Rev. B **19**, 2775 (1979).
[37] D. W. Oxtoby and A. D. J. Haymet, J. Chem. Phys. **76**, 6262 (1982).
[38] P. Tarazona, Mol. Phys. **52**, 871 (1984).
[39] Y. Singh, J. P. Stoessel, and P. G. Wolynes, Phys. Rev. Lett. **54**, 1059 (1985).
[40] H. Löwen, J. Phys.: Condens. Matter **2**, 8477 (1990).
[41] C. Kaur and S. P. Das, Phys. Rev. Lett. **86**, 2062 (2001).
[42] C. Dasgupta, Europhys. Lett. **20**, 131 (1992).
[43] T. Odagaki, T. Yoshidome, T. Tao, and A. Yoshimori, J. Chem. Phys. **117**, 10151 (2002).
[44] Y. Singh, Phys. Reps. **207**, 351 (1991).
[45] H. Löwen, Phys. Rep. B **237**, 249 (1994).

[46] N. W. Ashcroft, Aust. J. Phys. **49**, 3 (1996).
[47] J.-P. Hansen and J. R. McDonald, *Theory of Simple Liquids*, 2nd ed. (Academic Press, London, 1986).
[48] P. Tarazona, Phys. Rev. A **31**, 2672 (1985).
[49] M. S. Wertheim, J. Math. Phys. **5**, 643 (1964).
[50] E. Thiele, J. Chem. Phys. **39**, 474 (1963).
[51] J. K. Percus and G. J. Yevick, Phys. Rev. **110**, 1 (1958).
[52] J. D. Bernal, Proc. Roy. Soc. London Ser. A **280**, 299 (1964).
[53] G. Parisi and F. Zamponi, J. Chem. Phys. **123**, 144501 (2005).
[54] B. Coluzzi, G. Parisi, and P. Verrocchio, J. Chem. Phys. **112**, 2933 (2000).
[55] L. Verlet and J. J. Weiss, Phys. Rev. A **5**, 939 (1972).
[56] S. P. Das and J. W. Dufty, Phys. Rev. A **46**, 6371 (1992).
[57] J. F. Lutsko, J. W. Dufty, and S. P. Das, Phys. Rev. A **39**, 1311 (1989).
[58] S. P. Das and R. Schilling, Phys. Rev. E **50**, 1265 (1994).
[59] S. Srivastava and S. P. Das, Phys. Lett. A **286**, 76 (2001).
[60] Y. Rosenfeld, Phys. Rev. Lett. **63**, 980 (1989).
[61] Y. Rosenfeld, M. Schmidt, H. Löwen, and P. Tarazona, Phys. Rev. E **55**, 4245 (1997).
[62] V. Lubchenko and P. G. Wolynes, Annu. Rev. Phys. Chem. **58**, 235 (2007).
[63] R. W. Hall and P. G. Wolynes, Phys. Rev. Lett. **90**, 085505 (2003).
[64] R. W. Hall and P. G. Wolynes, J. Phys. Chem. B **112**, 301 (2008).
[65] P. Rabochiy and V. Lubchenko, J. Chem. Phys. **136**, 084504 (2012).
[66] C. Kaur and S. P. Das, Phys. Rev. E **65**, 026123 (2002).
[67] K. Kim and T. Munakata, Phys. Rev. E **68**, 021502 (2003).
[68] P. Chaudhuri, S. Karmakar, C. Dasgupta, H. R. Krishnamurthy, and A. K. Sood, Phys. Rev. Lett. **95**, 248301 (2005).
[69] S. L. Singh, A. S. Bharadwaj, and Y. Singh, Phys. Rev. E **83**, 051506 (2011).
[70] C. Bennett, J. Appl. Phys. **43**, 2727 (1972).